

Localization of double bonds in triacylglycerols using high-performance liquid chromatography/atmospheric pressure chemical ionization ion-trap mass spectrometry

Eva Háková · Vladimír Vrkoslav · Radka Míková ·
Karolina Schwarzová-Pecková · Zuzana Bosáková ·
Josef Cvačka

Received: 12 December 2014 / Revised: 28 January 2015 / Accepted: 5 February 2015 / Published online: 21 February 2015
© Springer-Verlag Berlin Heidelberg 2015

Abstract A method for localizing double bonds in triacylglycerols using high-performance liquid chromatography–tandem mass spectrometry with atmospheric pressure chemical ionization (APCI) was developed. The technique was based on collision-induced dissociation or pulsed Q collision-induced dissociation of the $C_3H_5N^{+}$ adducts ($[M + 55]^{+}$) formed in the presence of acetonitrile in the APCI source. The spectra were investigated using a large series of standards obtained from commercial sources and prepared by randomization. The fragmentation spectra made it possible to determine (i) the total number of carbons and double bonds in the molecule, (ii) the number of carbons and double bonds in acyls, (iii) the acyl in the *sn*-2 position on the glycerol backbone, and (iv) the double-bond positions in acyls. The double-bond positions were determined based on two types of fragments (alpha and omega ions) formed by cleavages of C–C bonds vinylic to the original double bond. The composition of the acyls and their positions on glycerol were established from

the masses and intensities of the ions formed by the elimination of fatty acids from the $[M + 55]^{+}$ precursor. The method was applied for the analysis of triacylglycerols in olive oil and vernix caseosa.

Keywords Double bond · Gas-phase chemistry · Lipidomics · Olive oil · Vernix caseosa

Introduction

Triacylglycerols (TGs) are the main storage lipids in animal and plant tissues and consequently they are the major fat in the human diet [1]. The TG molecules contain a glycerol backbone, to which three fatty acids are esterified; the variety of fatty acids distributed among the *sn*-1, *sn*-2, and *sn*-3 positions of glycerol often makes TG mixtures very rich. The structure of TGs affects their physico-chemical properties and metabolic fates. Therefore, analytical tools which make it possible to elucidate their molecular structures are of great importance for various branches of life science and industry.

A complete structural characterization of TGs in their mixtures is not an easy task. The molecular species of TGs typically need to be separated from each other before elucidating their structures. Chromatographic separations are mostly carried out in various systems based on (U)HPLC in reversed-phase [2–5], silver-ion [4, 6, 7], and chiral [8] modes. Because of entirely different separation mechanisms, they can be combined in 2D systems [9, 10]. Retention parameters are useful for TG characterization, especially when standards are available for comparison [11]. However, the structures of TGs are usually deduced from their mass spectra. Various methods are

Published in the topical collection *Lipidomics* with guest editor Michal Holčapek.

Electronic supplementary material The online version of this article (doi:10.1007/s00216-015-8537-1) contains supplementary material, which is available to authorized users.

E. Háková · R. Míková · K. Schwarzová-Pecková · Z. Bosáková
Department of Analytical Chemistry, Faculty of Science, Charles
University in Prague, Hlavova 2030/8, 128 43 Prague
2, Czech Republic

E. Háková · V. Vrkoslav · R. Míková · J. Cvačka (✉)
Institute of Organic Chemistry and Biochemistry v.v.i., Academy of
Sciences of the Czech Republic, Flemingovo nám. 2, 166 10 Prague
6, Czech Republic
e-mail: Cvačka@uochb.cas.cz

used for ionizing TGs, including electrospray ionization (ESI) [5, 12–14], atmospheric pressure chemical ionization (APCI) [2–4, 6, 7, 15], atmospheric pressure photoionization (APPI) [16], matrix-assisted laser desorption/ionization (MALDI) [17–19], desorption electrospray ionization (DESI) or desorption atmospheric pressure photoionization (DAPPI) [20], fast atom bombardment (FAB) [21], electron ionization (EI) [22], chemical ionization (CI), and field desorption (FD) [23]. Ionization methods permitting on-line coupling with liquid chromatography are more convenient and often indispensable for complex TG mixtures. The first-stage mass spectra usually provide information on molecular weight, i.e., the total number of carbons and double bonds in TG molecules. Depending on the ionization used, the spectra may already contain fragments useful for the structure elucidation, for instance ions formed by a neutral loss of fatty acids. In other cases, collision-induced dissociation (CID) of the molecular adducts or ions is used for the structure elucidation.

To date, several mass spectrometry-based strategies have been demonstrated for the localization of double bonds in TGs [12, 18, 21, 24–30]. In principle, a double bond can be localized either by direct fragmentation of unsaturated chains utilizing charge-remote fragmentation (CRF) channels, or by charge- or radical-driven fragmentations of specific products formed by reactions at the site of a double bond. The CRF of TGs can be achieved using high-energy CID on double-focusing or four-sector mass spectrometers and tandem time-of-flight instruments [18, 21]. Molecular adducts with ammonium ions or sodium ions generated by ESI, FAB, or MALDI and activated at several keV provide a series of CRF ions by the elimination of C_nH_{2n+1} and C_nH_{2n+2} from the precursor ions. The double bond in the chain becomes evident from the irregularities of the CRF-ion intensities. The CRF can also be achieved using low-energy CID in triple quads and ion traps utilizing lithium adducts of TGs [12, 27]. In the fundamentally different approaches, TGs are chemically derivatized on the double bond to create products that provide fragments indicating the original position of the double bond. Such reactions are preferably performed in the gas phase. A reaction with ozone introduced into an electrospray ion source (OzESI-MS) has been used for an on-line analysis of unsaturated TGs [24]. Ozone-induced fragments bearing an aldehyde and an α -methoxyhydroperoxide group enabled the localization of a double bond. The method was later modified and the reaction was carried out in an ion-trap analyzer with mass-selected precursors (OzID) [26], which was also effective for the identification of double-bond positions in polyunsaturated TGs [28]. Radical-driven fragmentations promote intrachain cleavages, which can also be used for localizing double bonds in TGs. This approach has recently been demonstrated using bifunctional reagents containing a lipid-adducting group and a photocaged radical initiator such as 4-iodoaniline [30]. The reagent is noncovalently attached to a TG molecule; the

adduct is isolated in an ion trap and irradiated by a UV laser. The nascent radical unmasked by photodissociation presumably adds to the double bond of TG. Subsequent CID of the product gives rise to radical-directed dissociation of the unsaturated acyl chains.

The double bonds in lipids can also be localized using gas-phase chemistry of acetonitrile. These approaches are potentially advantageous and convenient for TGs, because acetonitrile is commonly used in mobile phases for HPLC separations and the reactions can be performed directly in the APCI sources. Common mass spectrometers without any modification can be used for this purpose. The acetonitrile gas-phase reactions were initially utilized for the localization of double bonds in CI mass spectrometry [31–43]. The lipids reacted with (1-methylenimino)-1-ethenyl cation ($C_3H_4N^+$) generated by an ion-molecule reaction between $C_2H_2N^+$ and neutral acetonitrile [32, 44]. The $[M + C_3H_4N]^+$ covalent adduct formed by a [2+2]cycloaddition reaction provided fragments indicative for the position of a double bond [35]. The method was mostly applied for fatty acid methyl esters (FAMEs), including methylene-interrupted and non-methylene-interrupted polyunsaturated FAMEs [35–43]. This approach has also been adapted for APCI and applied for monoene- and diene-containing TGs [25]. Similarly to CI, the $C_3H_4N^+$ ions reacted with unsaturated TGs, yielding $[M + 54]^+$ covalent adducts. The CID of $[M + 54]^+$ in a triple-quadrupole linear ion trap provided ions corresponding to cleavage either vinylic or allylic to the site of the double bond. Other acetonitrile-related adducts, namely $[M + 40]^+$, $[M + 81]^+$, and $[M + 95]^+$, were formed as well, and these ions were also useful for the localization of double bonds. We have previously demonstrated the use of APCI and acetonitrile gas-phase chemistry for the localization of double bonds in various unsaturated neutral lipids [29, 45, 46]. For the investigated lipids, we have observed the formation of radical cations $[M + 55]^{+•}$ ($[M + C_3H_5N]^+$) rather than $[M + 54]^+$ ($[M + C_3H_4N]^+$), described for TGs [25]. When fragmented by CID, the $[M + 55]^{+•}$ provided useful diagnostic fragments for the localization of double bonds [29, 45, 46]. Moreover, the ion-source conditions were fully compatible with the high flow rates of solvents typically used for HPLC/APCI-MS.

Here, we discuss the advantages and limitations of the localization of double bonds in TGs using ion-trap CID and pulsed Q collision-induced dissociation (PQD) of $[M + 55]^{+•}$ formed in the presence of acetonitrile. The CID and PQD fragmentation spectra were measured for a large series of TG standards differing by the number, position, and geometry of double bonds to investigate the usefulness of this approach. The spectra obtained in this way were compiled into an annotated library with 125 entries. The existing methods for the analysis of TGs based on HPLC/APCI-MS have been modified by adding a fragmentation step to obtain additional information on the double-bond position. The practicability of

these methods was demonstrated for olive oil and unsaturated TGs from vernix caseosa.

Material and methods

Chemicals and reagents

MS grade acetonitrile and propan-2-ol (Sigma Aldrich, St. Louis, MO, USA) were used as received. The other solvents (chloroform, hexane, diethyl ether; all from Penta, Czech Republic) were distilled in glass from analytical-grade solvents. Sodium methoxide and Rhodamine 6G were from Sigma Aldrich; 4',5'-dichlorofluorescein was purchased from Fluka (Buchs, Switzerland). The TG standards (purity: 99 %) were obtained from Nu-Chek-Prep (Elysian, MN, USA) and their standard solutions were prepared in chloroform (20 µg/mL).

Synthesis of TGs by randomization

The randomization (interesterification) procedure [7] was downscaled as follows: two standards of TGs (5 mg of each) and sodium methoxide (5 mg) were weighed into a dry glass ampoule. Hexane (200 µL) dried over molecular sieves (4 Å, pellets 3.2 mm, Sigma Aldrich, USA) was added, the ampoule was sealed and heated in a water bath at 80 °C for 30 min. Randomized TGs were isolated by semi-preparative thin-layer chromatography (TLC) on glass plates (36 mm × 76 mm) coated with 0.2 mm of Adsorbosil-Plus (Applied Science Labs; with gypsum (12 %)) using hexane/diethyl ether (80:20, v/v) mobile phase. TLC zones were made visible by spraying Rhodamine 6G solution (0.05 % in ethanol). A zone corresponding to TGs ($R_f=0.45-0.55$) was scraped off the plate and extracted with freshly distilled diethyl ether. The solvent was evaporated to dryness under nitrogen stream. The randomized TGs were reconstituted in chloroform (300–500 µg/mL).

Samples of natural TGs

Olive oil (extra virgin, Frantoio Larocca, Italy) was dissolved in acetonitrile/propan-2-ol/hexane (1:1:1, v/v/v) at a concentration of 10 mg/mL and used without any further purification. Vernix caseosa was obtained from a healthy female subject delivered at full term. The sample was collected with a written informed parental consent and the work was approved by the Ethics Committee of the General University Hospital, Prague (910/09S-IV). Vernix caseosa (1 g) was suspended in 50 mL of chloroform:methanol (2:1, v/v) with 0.05 % of 2,6-di-*tert*-butyl-4-methylphenol. The suspension was filtered, treated with anhydrous MgSO₄ to eliminate water, and filtered again. The solvents were removed by a rotary evaporator and the total lipid extract (20 mg) was separated on 90 mm ×

120 mm glass TLC plates coated with a 0.2 mm layer of silica gel 60 G (Merck, Darmstadt, Germany) using hexane:diethyl ether (93:7, v/v) as a mobile phase. The plate was developed twice to focus the zones (in the first step to 3/4 of the plate height and then, after air-drying, to the top). The zone corresponding to TGs ($R_f=0.19-0.27$; identical with R_f of triolein) was scraped off into a column with purified cotton-wool. Lipids were eluted with diethyl ether and the solvent was evaporated under a stream of argon. Vernix caseosa TGs were further separated using argentation TLC to obtain a fraction of unsaturated TGs. Argentation TLC was performed on glass plates (36 mm × 76 mm) coated with a 0.2 mm layer of silica gel with 10 % of silver nitrate (Sigma) and 12 % of gypsum. The mobile phase consisted of chloroform:methanol (99:1, v/v). The zone of unsaturated TGs ($R_f=0.35-0.83$) visualized under UV light after the plates were sprayed with 4',5'-dichlorofluorescein (0.1 % in methanol) was scraped off the plates and extracted with chloroform. The solvent was evaporated and TGs were reconstituted in chloroform at a concentration of 3.0 mg/mL.

APCI-MS and HPLC/APCI-MS

The experiments were performed using a system consisting of a Rheos Allegro UHPLC pump, an Accela autosampler with an integrated column oven and a LCQ Fleet ion-trap mass spectrometer equipped with an APCI source; the system was controlled by Xcalibur software (all provided by Thermo Fisher Scientific, San Jose, CA, USA). For direct infusion experiments, TGs dissolved in chloroform (20 µg/mL for commercial standards; 300–500 µg/mL for randomized TGs) were delivered by a syringe pump (a flow rate of 20 µL/min) to a low-dead-volume T-piece, where they were mixed with the mobile phase (acetonitrile, 0.5 mL/min). The APCI vaporizer and heated capillary temperatures were set to 250 and 180 °C, respectively. Nitrogen served both as the sheath and auxiliary gas at a flow rate of 60 and 45 arbitrary units, respectively. The MS spectra of the positively charged ions were recorded from 250 to 1050 *m/z*. The precursors were selected with an isolation width of 0.4–2.4 Da and fragmented using CID or PQD; the mass spectra were averaged from 2–10-min records. The TG mixtures were separated using Nova-Pak C18 columns (300+150 mm × 3.9 mm, particle size: 4 µm; Waters, Milford, MA, USA) with a C18 pre-column (4 mm × 2 mm, Phenomenex, USA) at 30 °C. The gradient program for olive oil: 0 min: 100 % acetonitrile; 106 min: 31 % acetonitrile/69 % propan-2-ol; 109 min: 100 % acetonitrile [47]; the mobile-phase flow rate was 0.8 mL/min and the injected volume of the sample was 10 µL. The gradient program for vernix caseosa TGs: 0 min: 100 % acetonitrile, 0.8 mL/min; 99 min: 34 % acetonitrile/66 % propan-2-ol, 0.8 mL/min; 114.5 min: 24 % acetonitrile/76 % propan-2-ol, 0.55 mL/min; 142 min: 5 % acetonitrile/95 % propan-2-ol, 0.3 mL/min.

min; 165 min: 5 % acetonitrile/95 % propan-2-ol, 0.3 mL/min; the injected volume of the sample was 25 μ L. The flow rate of the mobile phase had to be lowered in the course of the analysis to avoid excessive column back pressure at high concentrations of propan-2-ol. The CID MS² spectra of $[M + 55]^{++}$ were collected using data-dependent analysis with an isolation width of 2 Da and a normalized collision energy of 33–34 %. The masses of the acetonitrile adducts for fragmentation were calculated as higher partners of the base peaks (m/z of $[M + H]^+ + 54$ Da).

The nomenclature and notation of fragment ions

The TGs in this work are abbreviated as “TG” followed by three fatty acyls expressed as the number of carbon atoms: the number of double bonds. The fatty acyls are separated either by an underscore character (when their positions are not known or when they are distributed randomly) or by a slash (when the positions are proven) [48]. The positions of the double bonds are given in the $n-x$ nomenclature. Unless stated otherwise, *cis* double-bond geometry and methylene-interrupted double bonds in polyunsaturated chains are assumed. Thus, for instance, “TG 18:1($n-9$)/16:0/16:0” indicates 1-oleoyl-2,3-dipalmitoyl-glycerol or 1-olein-2,3-dipalmitin. The fragments of $[M + 55]^{++}$ originated by the cleavages of the C–C bonds next to the double bond are labeled as “ α ” if they contain ester moieties, or “ ω ” if they carry the terminal-carbon end and do not include an ester group. If needed, “ α ” and “ ω ” fragments have been specified with a subscript indicating a double bond within a chain and/or by a superscript indicating the chain within a TG. For instance, $\alpha_{n-6}^{18:2}$ refers to an α fragment corresponding to an $n-6$ double bond on an 18:2 acyl in a TG. The ECN stands for the equivalent carbon number (ECN=CN-2DB, where CN and DB are the total numbers of the carbon atoms and double bonds, respectively).

Results and discussion

The preparation of TGs with randomized acyls

The offer of commercially available TG standards is limited mostly to monoacid TGs having the same acyls in all three glycerol positions. In order to study the mass spectra of structurally diverse TGs occurring in nature, we prepared a set of standards using chemical interesterification, also called randomization [49]. This process causes fatty-acid redistribution within and among TG molecules according to the laws of probability. The randomization reactions were performed with two monoacid TGs (AAA, BBB) having up to six double bonds in acyls. This made it possible to obtain mixtures of TGs combining two fatty acyls. Besides the reactants (AAA,

BBB), two new signals appeared in the APCI spectra of the randomized samples: the first one for regioisomers with one “A” chain and two “B” chains (ABB, BBA, BAB) and the second representing regioisomers with two “A” chains and one “B” chain (BAA, AAB, ABA). The randomized TGs were used for MS² experiments directly, without their chromatographic separation. In compliance with the nomenclature used in this work, the randomized standards were abbreviated with underscore separators (i.e., TG A_B_B or TG B_A_A).

The formation of $[M + 55]^{++}$ ions

As already discussed in our previous work [29], direct infusion of unsaturated TGs into the APCI source in the presence of acetonitrile promoted the formation of acetonitrile-related adducts. For instance, 1,2-palmitin-3-olein (TG 16:0/16:0/18:1($n-9$)) provided a spectrum shown in Fig. 1a. The acetonitrile-related adducts were observed at m/z 871.6 ($[M + 39]^+$), m/z 874.0 ($[M + 41]^{++}$; likely with a contribution of $[M + 42]^+$, as the mass was slightly shifted), m/z 887.4 ($[M + 55]^{++}$), m/z 913.5 ($[M + 81]^+$) and m/z 927.4 ($[M + 95]^+$). The relative intensity of the acetonitrile-related adducts varied depending on the TG structure as well as the settings of the ion source. For instance, the $[M + 41]^{++}$ ion (not useful for the localization of double bonds in TGs) was highly abundant in the spectra of TGs with monounsaturated chains and low for polyunsaturated TGs. Lowering the acetonitrile flow rate significantly decreased the formation of this ion. Concerning the $[M + 55]^{++}$, monounsaturated TGs provided somewhat more abundant signals than the polyunsaturated species and the ion intensity was not significantly dependent on the acetonitrile flow rate. The intensities of $[M + 55]^{++}$ were rather low, typically 1–5 % with regard to $[M + H]^+$. Our attempts to increase the signal intensity by changing the ion-source parameters were successful only partially; higher $[M + 55]^{++}$ signals were achieved at lower vaporizer temperature with the optimum around 250 °C. Despite the relatively low abundance of $[M + 55]^{++}$, the quality of the MS/MS spectra was generally good.

The other peaks in the spectrum shown in Fig. 1a corresponded to a protonated molecule (m/z 833.4) and diacylglycerol fragments originated after the loss of oleic acid (m/z 551.4) and palmitic acid (m/z 577.4).

MS² of $[M + 55]^{++}$: TGs with monounsaturated chains

The MS² spectra of the $[M + 55]^{++}$ ions were investigated for a large series of TGs obtained from commercial sources or prepared by randomization reactions. The resonance excitation CID mass spectrum of 1,2-palmitin-3-olein is shown in Fig. 1b. The spectrum basepeak at m/z 774.4 was an α fragment formed by the cleavage of the C–C bond vinylic to the original double bond. A neutral loss of palmitic acid from the precursor yielded m/z 631.5 ($[M + 55-FA_{16:0}]^{++}$). Note that a

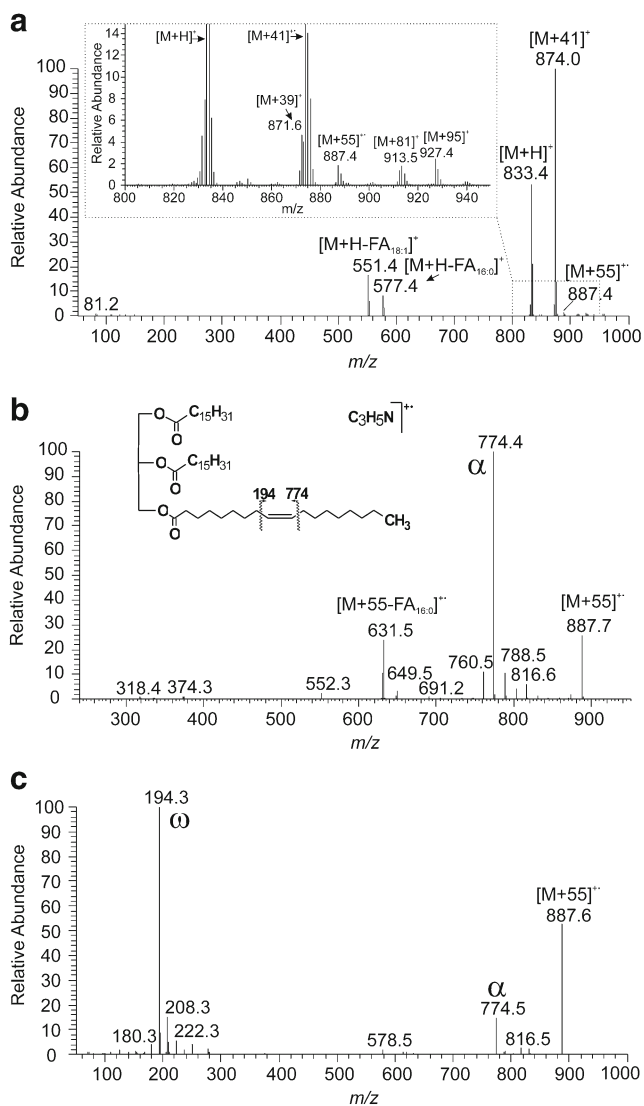


Fig. 1 The full-scan APCI mass spectrum (**a**), the APCI CID MS² spectrum of the $[M + 55]^{++}$ adduct (**b**) and the APCI PQD MS² spectrum of the $[M + 55]^{++}$ adduct (**c**) of TG 16:0/16:0/18:1(*n*-9) (1,2-palmitin-3-olein). The standard solution (20 μ g/mL in chloroform) delivered by a syringe pump (20 μ L/min) was mixed in a T-piece with acetonitrile (0.5 mL/min) and infused into the ion source (the spectra averaged from 0.5-, 2.0-, and 4.0-min records, respectively)

neutral loss of oleic acid was not observed, obviously because oleyl was covalently modified with $C_3H_5N^{++}$. The diagnostic fragment formed by a cleavage of the C–C bond on the opposite side of the original double bond (ω fragment) was not detected because of the low-mass cut-off of the ion trap. This problem can be circumvented with PQD, which activates ions at high Q values and collects fragments at low Q values, resulting in spectra similar to CID containing also low m/z fragments. PQD also helps to access higher-energy dissociation channels. The main drawback of PQD is less effective ion fragmentation relative to CID, which results in spectra of lower overall intensities. A PQD spectrum of 1,2-palmitin-3-olein

is shown in Fig. 1c; both diagnostic fragments were detected (α at m/z 774.5 and ω at m/z 194.3). The spectra also showed smaller peaks accompanying the α and ω fragments (14 Da difference; $\pm(CH_2)_n$) created by less probable cleavages of the more distant C–C bonds with regard to the double bond. Although PQD provided both diagnostic fragments and the CID only one, both types of activation afforded spectra allowing for an unambiguous assignment of the double bond to the *n*-9 position on the 18:1 chain. A regioisomer 1,3-dipalmitin-2-olein (TG 16:0/18:1(*n*-9)/16:0) provided very similar spectra, with slightly modified ion abundances (Spectrum S7). The spectra of other TGs with one monounsaturated acyl (see more examples in the [Electronic Supplementary Material \(ESM\)](#)) provided analogous spectra, facilitating straightforward localization of the double bond.

The MS² spectra of TGs with two or three identical monounsaturated chains were found to be analogous to the previously discussed ones. The covalent attachment of $C_3H_5N^{++}$ occurred randomly on one of the unsaturated chains and the remaining chains stayed unmodified. For instance, CID of 1, 3-olein-2-palmitin (TG 18:1(*n*-9)/16:0/18:1(*n*-9)), see Fig. 2a, provided mainly an α ion at m/z 800.5 and fragments consistent with the neutral loss of palmitic acid (m/z 657.2; $[M + 55-FA_{16:0}]^{++}$) and oleic acid (m/z 631.5; $[M + 55-FA_{18:1}]^{++}$). The CID of triolein (TG 18:1(*n*-9)/18:1(*n*-9)/18:1(*n*-9)) provided an α fragment at m/z 826.5 and $[M + 55-FA_{18:1}]^{++}$ at m/z 657.6 (Fig. 2b). The PQD MS² spectrum of triolein (Fig. 2c) showed also an ω fragment at m/z 194.3 and relatively high abundant ions at m/z 318.4 and m/z 332.5. These fragments, which are not straightforward to rationalize, were also present as small peaks in the CID spectrum (Fig. 2b). We speculate that these fragments did not originate from a precursor with just one double bond modified with $C_3H_5N^{++}$ but rather from a cross-linked precursor, where $C_3H_5N^{++}$ bridges two double bonds on neighboring chains. The fragments might be rationalized by C–C bond cleavages at the positions which are vinylic to the site of the former double bonds on both chains (m/z 332.5) and cleavages yielding a product that is one methylene group shorter (m/z 318.4). Hence, the masses of these even electron products containing a nitrogen atom but no oxygen must depend on the positions of double bonds. This was indeed observed in the spectra of other monoacid TGs containing C18:1 acyls with different double-bond positions. The above-mentioned fragments were shifted by 56 Da (4 methylene units) towards lower m/z values in trivaccenin (TG 18:1(*n*-7)/18:1(*n*-7)/18:1(*n*-7)), see Spectrum S32, and by 84 Da (6 methylene units) towards higher m/z values in tripetroselinin (TG 18:1(*n*-12)/18:1(*n*-12)/18:1(*n*-12)), see Spectrum S28. No shifts of the fragment masses were observed in the spectrum of trielaidin (TG 18:1(*n*-9 t)/18:1(*n*-9 t)/18:1(*n*-9 t)), see Spectrum S31, which has double bonds at the same positions as triolein, but their geometry is *trans*. Unfortunately, we were not able to record MS³ spectra

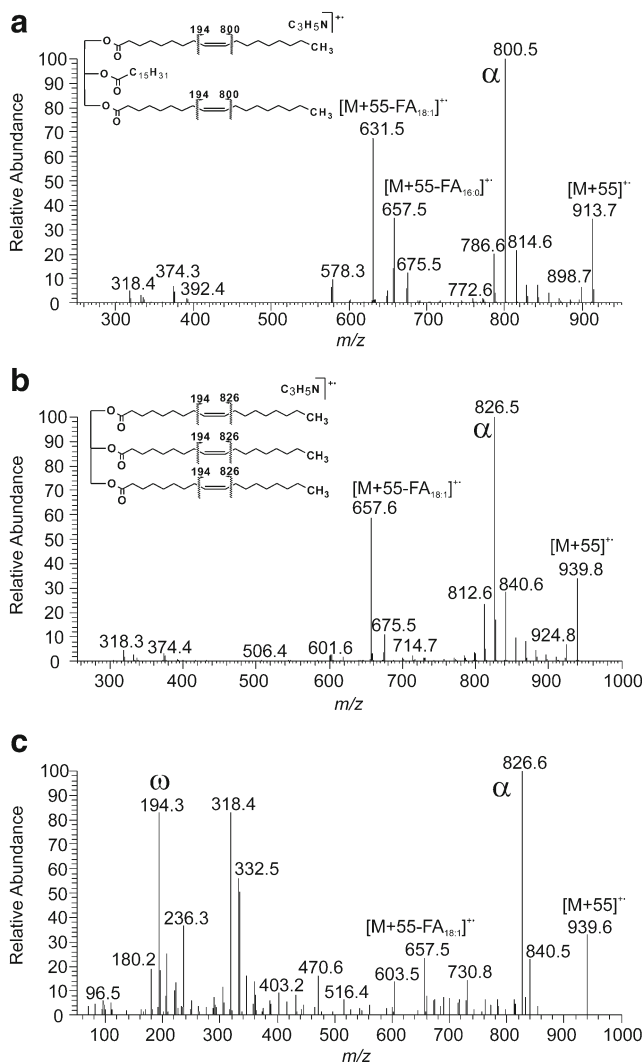


Fig. 2 The APCI CID MS² spectrum of the [M + 55]⁺⁺ adduct of TG 18:1(*n*-9)/16:0/18:1(*n*-9) (1,3-olein-2-palmitin) (a) and 18:1(*n*-9)/18:1(*n*-9)/18:1(*n*-9) (triolein) (b). The APCI PQD MS² spectrum of the [M + 55]⁺⁺ adduct of TG 18:1(*n*-9)/18:1(*n*-9)/18:1(*n*-9) (triolein) (c). The standard solution (20 μg/mL in chloroform) delivered by a syringe pump (20 μL/min) was mixed in a T-piece with acetonitrile (0.5 mL/min) and infused into the ion source (the spectra averaged from a 2-min record)

and reliably measure the exact masses to confirm our hypothesis further.

The fragmentation spectra were noticeably different for TGs with the double bond located at the chain terminus (*n*-1 position). In the CID spectrum of triundecenoin (TG 11:1(*n*-1)/11:1(*n*-1)/11:1(*n*-1)) (Fig. 3a), the most abundant fragment at *m/z* 630.5 corresponded to the loss of methyl radical. The PQD spectrum (Fig. 3b) showed *m/z* 96.2 as a basepeak, indicating C-C bond cleavage at a position that is allylic to the site of the former double bond. Analogous diagnostic fragments ([M + 55-CH₃]⁺ and *m/z* 96) were also found in the randomized TGs with one or two 10*Z*-undecenoyls (Spectra S1, S11, S107, and S111).

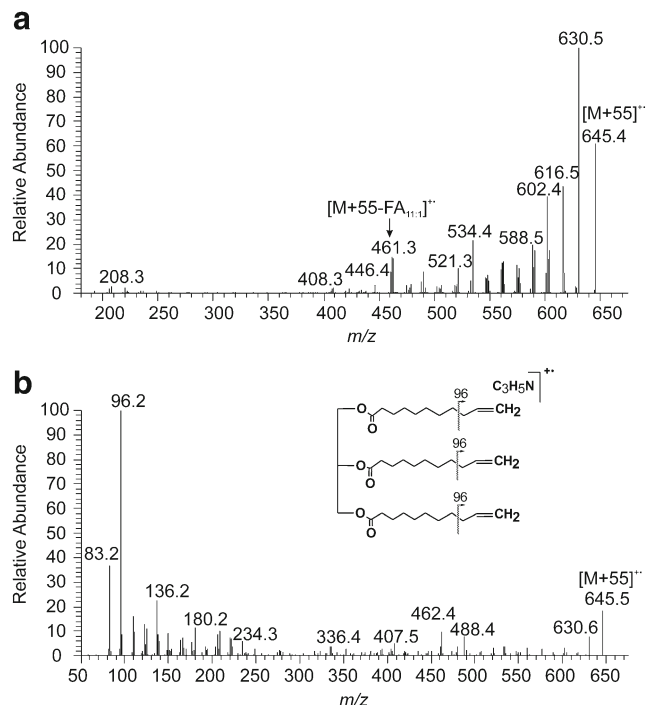


Fig. 3 The APCI CID (a) and PQD (b) MS² spectra of the [M + 55]⁺⁺ adduct of TG 11:1(*n*-1)/11:1(*n*-1)/11:1(*n*-1) (triundecenoin). The standard solution (20 μg/mL in chloroform) delivered by a syringe pump (20 μL/min) was mixed in a T-piece with acetonitrile (0.5 mL/min) and infused into the ion source (the spectra averaged from 3- and 5-min records, respectively)

As regards the double-bond geometry, no significant differences between fragmentation spectra were observed. The ion abundances were similar for the *cis* and *trans* isomers, see Spectra S2/S3 and S4/S5.

In all TGs with one or more identical monounsaturated chains, the diagnostic fragments reliably and unambiguously indicated the position of double bond(s). However, TGs can consist of two or three monounsaturated chains with different positions of the double bond. For such TGs, the MS² spectra did not allow the assignment of the double-bond position to a particular chain. In principle, MS³ spectra can be used in these cases. In diolein-palmitolein (TG 18:1(*n*-9)_18:1(*n*-9)_16:1(*n*-7)), for instance, two α ions were recorded: α_{*n*-7} at *m/z* 826.4 and α_{*n*-9} at *m/z* 798.6 (Fig. 4a). We, of course, know that the palmitoleyl has an *n*-7 double bond and the oleyl an *n*-9 double bond, but one cannot say that from the spectrum. Supposedly, MS³ of the α ions should show a neutral loss of 18:1 acid (if we fragment an ion derivatized on the 16:1 chain) or a loss of both 16:1 and 18:1 acids (if we fragment an ion derivatized on the 18:1 chain). This is indeed true; the fragmentation of α_{*n*-9} gives [α_{*n*-9}-FA_{18:1}]⁺ (*m/z* 516.5) and [α_{*n*-9}-FA_{16:1}]⁺ (*m/z* 544.5) (Fig. 4b), whereas the fragmentation of α_{*n*-7} gives mostly [α_{*n*-7}-FA_{18:1}]⁺ (*m/z* 544.5) (Fig. 4c). Therefore, an *n*-7 double bond must be in a 16:1 chain, whereas an *n*-9 double bond in an 18:1 chain. However, this approach was found to be somewhat limited by low specificity. In the MS³ spectrum of α_{*n*-7}, we also detected a small but

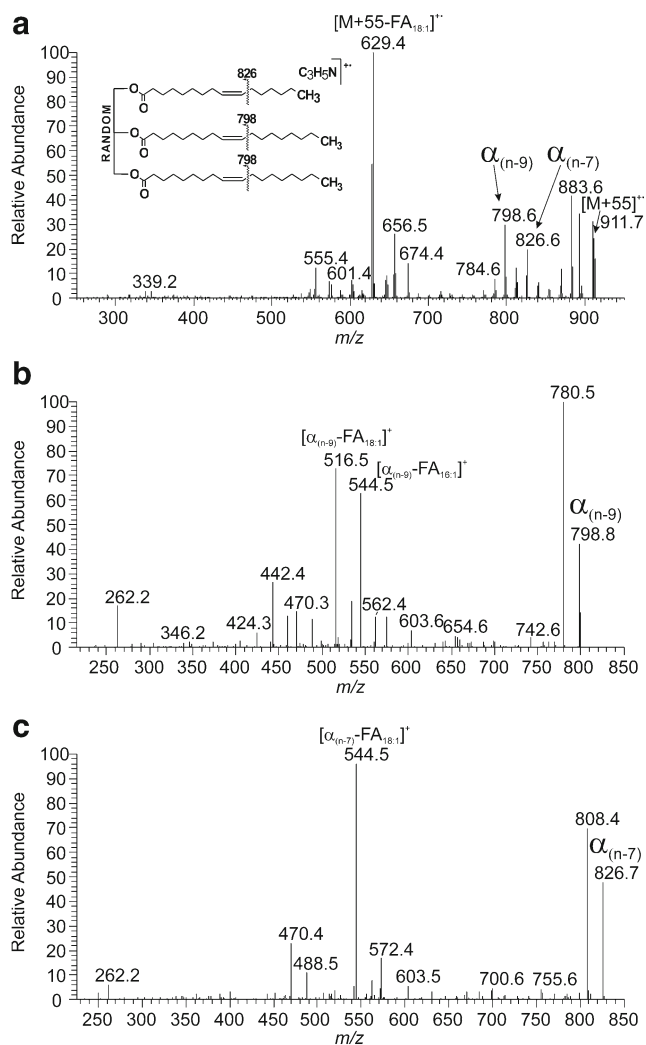


Fig. 4 The APCI CID MS² spectrum of the $[M + 55]^{+}$ adduct of TG 18:1(*n*-9)₂:18:1(*n*-9)₂:16:1(*n*-7) (**a**), the MS³ spectrum of α ions corresponding to the *n*-9 double bond (911.9 \rightarrow 798.6) (**b**) and the MS³ spectrum of α ions corresponding to the *n*-7 double bond (911.9 \rightarrow 826.5) (**c**). The standard solution (20 μ g/mL in chloroform) delivered by a syringe pump (20 μ L/min) was mixed in a T-piece with acetonitrile (0.5 mL/min) and infused into the ion source (the spectra averaged from a 2-min record)

significant peak $[\alpha_{n-7}\text{-FA}_{16:1}]^{+}$ (*m/z* 572.4), which in theory should not be formed. The presence of this peak can be explained by (i) the co-isolation of an α -like ion derivatized on the 18:1 chain but cleaved in a propenyl C–C bond or (ii) the scrambling or migration of the $\text{C}_3\text{H}_5\text{N}^{+}$ modification. The MS³ spectra of $[M + 55\text{-FA}]^{+}$ also provided fragments indicating the double-bond positions (analogous to α fragments; the loss of hydrocarbon radical), but at unusably low intensities.

MS² of $[M + 55]^{+}$: TGs with di- and polyunsaturated chains

With the increasing number of double bonds in acyls, the fragmentation spectra of $[M + 55]^{+}$ become more complex. The covalent adduct formation took place on each double bond of

the chains, which increased the structural variability of the $[M + 55]^{+}$ precursors. Upon fragmentation, each double bond-site provided specific fragments (cleavages vinylic (or allylic) to the site of the double bond), together with unspecific fragments (cleavages on more distant C–C bonds from the site of the double bond). Consequently, the diagnostic ions became less pronounced and somewhat hidden among other fragments. We have noticed that the efficiency of adduct formation (or cleavage) depends on the double-bond position. Thus, for instance, the spectrum of distearin-linolein (TG 18:0₂:18:2(*n*-6)) showed a significantly more abundant α -ion corresponding to the *n*-6 double bond (α_{n-6} at *m/z* 866.5) when compared to the α -ion corresponding to the *n*-9 double bond (α_{n-9} at *m/z* 826.6) (Fig. 5a). It can be explained by the easier accessibility of the double bonds closer to the chain termini and/or by electronic effects. The same trend was also observed for other TGs with polyunsaturated chains, see for instance distearin- α -linolenin (TG 18:0₂:18:3(*n*-3)), Spectrum S21. For all three identical polyunsaturated acyl chains, the diagnostic fragments were easier to distinguish among other ions, like in the case of trilinolein (TG 18:2(*n*-6)/18:2(*n*-6)/18:2(*n*-6)), see Fig. 5b. Although the intensities of α and ω ions generally decreased with the distance of the double bond from the unsaturated chain terminus, some TGs showed enhanced intensities of α ions corresponding to the second (or third) double bond counting from the chain terminus (see for instance tri- α -linolenin, Spectrum S87). The most polyunsaturated TG investigated in this work was tridocosahexaenoic (TG 22:6(*n*-3)/22:6(*n*-3)/22:6(*n*-3)), Fig. 5c. Even in this compound, the α -ions corresponding to all double bonds were relatively easily recognizable. We can conclude that the localization of double bonds in TGs with one or more identical di- and polyunsaturated chains can be achieved. At least, the double bonds close to chain termini provided signals reliably indicating their positions.

The spectra of TGs with all the acyls unsaturated and/or polyunsaturated in various positions were challenging to interpret. The intensities of diagnostic ions indicating double bonds closer to glycerol in polyunsaturated chains were significantly suppressed. The spectra usually clearly showed only diagnostic ions corresponding to a double bond in the monounsaturated chain(s) and the outermost double bond in polyunsaturated chain(s). For instance, in the CID spectrum of dipetroselinin-linolelaidin (TG 18:1(*n*-12)₂:18:1(*n*-12)₂:18:2(*n*-6 t)), Fig. 6a, the double bond on the monounsaturated petroselinyl chain provided easily distinguishable $\alpha_{n-12}^{18:1}$ at *m/z* 782.6, similarly to the *n*-6 double bond in the diunsaturated linolelaidinyl chain ($\alpha_{n-6}^{18:2}$ at *m/z* 866.7). The $\alpha_{n-9}^{18:2}$ ion reflecting the *n*-9 double bond in the linolelaidinyl chain was detected at *m/z* 826.6, but its intensity did not exceed the surrounding ions. The polyunsaturated chains frequently contain double bonds on the same positions counting from the chain termini ("*n*-3" or "*n*-6" fatty chains). In these cases, the diagnostic fragments had the same mass and their intensities were enhanced. For

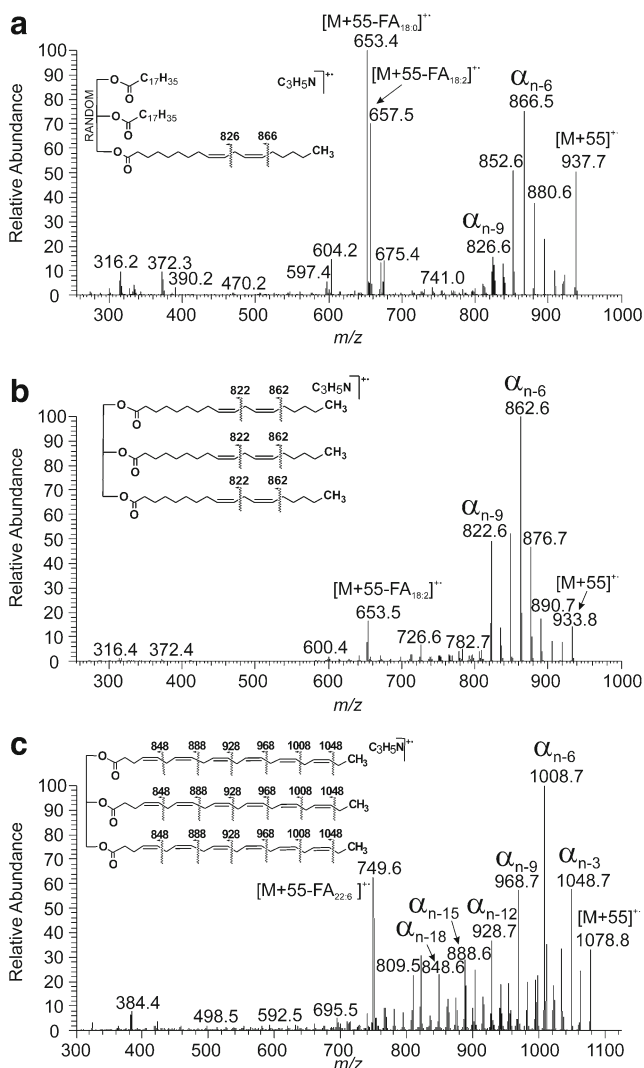


Fig. 5 The APCI CID MS² spectra of the [M + 55]⁺ adduct of distearin-linolein (TG 18:0_18:0_18:2(*n*-6)) (a), trilinolein (TG 18:2(*n*-6)/18:2(*n*-6)_18:2(*n*-6)) (b) and tridocosahexaenoin (TG 22:6(*n*-3)/22:6(*n*-3)/22:6(*n*-3)) (c). The standard solution (20 μg/mL in chloroform) delivered by a syringe pump (20 μL/min) was mixed in a T-piece with acetonitrile (0.5 mL/min) and infused into the ion source (the spectra averaged from 4-, 2-, and 2-min records, respectively)

instance, the α fragments in di-α-linolenin-docosahexaenoin (TG 18:3(*n*-3)_18:3(*n*-3)_22:6(*n*-3)) were for all chains at the same *m/z* values (α_{*n*-3}^{22:6} and α_{*n*-3}^{18:3} at *m/z* 948.7; α_{*n*-6}^{22:6} and α_{*n*-6}^{18:3} at *m/z* 908.7; α_{*n*-9}^{22:6} and α_{*n*-9}^{18:3} at *m/z* 868.7), see Fig. 6b. The remaining (inner) double bonds on docosahexaenoyls provided small α fragments almost indistinguishable from the background.

Fragment intensity ratio in regioisomers

The intensities of the diacylglycerol fragments in the APCI mass spectra of TGs ([M + H-RCOOH]⁺) are known to indicate acyl positions on the glycerol [50]. The elimination of

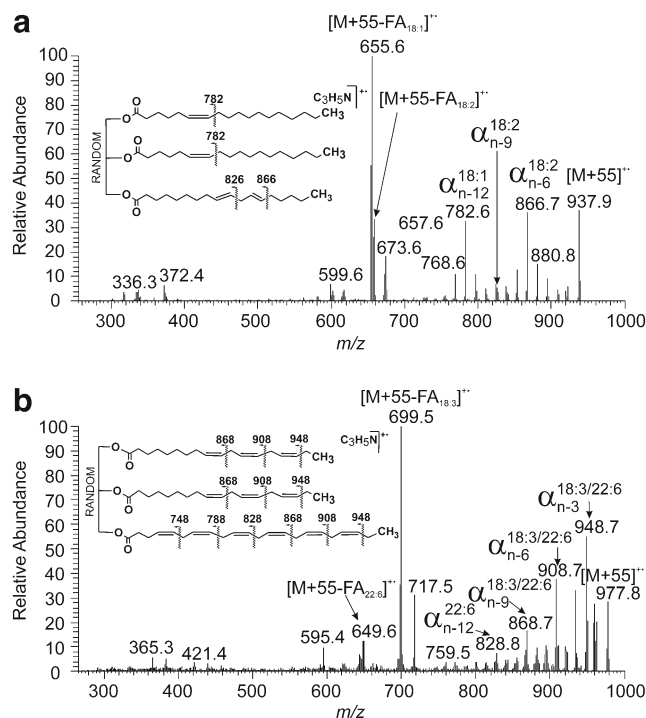


Fig. 6 The APCI CID MS² spectra of the [M + 55]⁺ adduct of dipetroselinin-linolelaidin (TG 18:1(*n*-12)_18:1(*n*-12)_18:2(*n*-6 t)) (a) and di-α-linolenin-docosahexaenoin (TG 18:3(*n*-3)_18:3(*n*-3)_22:6(*n*-3)) (b). The standard solution (20 μg/mL in chloroform) delivered by a syringe pump (20 μL/min) was mixed in a T-piece with acetonitrile (0.5 mL/min) and infused into the ion source (the spectrum averaged from a 5-min record)

fatty acids from the *sn*-1 and *sn*-3 positions is more likely and equally favored, whereas the fatty acid in the *sn*-2 position is less probable to cleave (the corresponding fragment is the least intense). Therefore, one can distinguish the acyl in the *sn*-2 position from those attached to the *sn*-1/*sn*-3 positions by comparing the fragment intensities. It is important to note that the fragment intensities are also affected by the chain-length and the degree of unsaturation of the cleaving fatty acid, which can lead to an incorrect assignment of the chain positions in some cases [51, 52]. Our results have indicated that the elimination of fatty acid in *sn*-2 position is less probable also in the case of the CID of [M + 55]⁺. Hence, the intensities of the [M + 55-FA]⁺ fragments could be useful for the acyl-position assignment like the intensities of the [M + H-FA]⁺ ions in the APCI full-scan mass spectra. However, the intensities of [M + 55-FA]⁺ cannot be used exactly in the same way as the intensities of [M + H-FA]⁺, because the acyl with the double bond modification is not cleaved. To test the hypothesis, the MS² spectra of [M + 55]⁺ were repeatedly measured for TG regioisomers and the ratios of the fragments were calculated (Table 1). Figure 7 shows zoomed spectral regions with fragments of 1-arachidin-2-olein-3-palmitin (TG 20:0/18:1(*n*-9)/16:0; AOP) and 1-palmitin-2-arachidin-3-olein (TG 16:0/20:0/18:1(*n*-9); PAO) regioisomers. The oleyl chain

Table 1 The ratio of the $[M + 55\text{-FA}]^{+}$ -fragment intensities in the CID MS² spectra of isomeric TGs

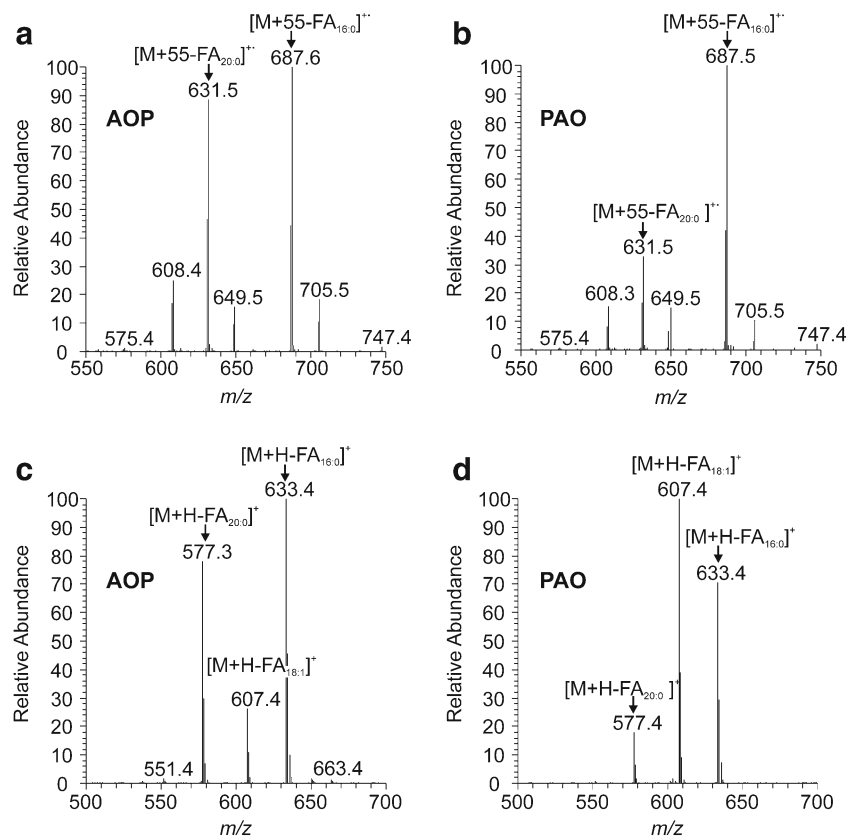
TG	Fragment no. 1	Fragment no. 2	Fragment intensity ratio Frg. 1/Frg. 2 ^a
TG 18:1(<i>n</i> -9)/16:0/18:1(<i>n</i> -9)	$[M + 55\text{-FA}_{18:1}]^{+}$	$[M + 55\text{-FA}_{16:0}]^{+}$	1.7±0.1
TG 18:1(<i>n</i> -9)/18:1(<i>n</i> -9)/16:0			0.4±0.0
TG 20:0/18:1(<i>n</i> -9)/16:0	$[M + 55\text{-FA}_{20:0}]^{+}$	$[M + 55\text{-FA}_{16:0}]^{+}$	0.8±0.0
TG 16:0/20:0/18:1(<i>n</i> -9)			0.3±0.0
TG 18:1(<i>n</i> -9)/18:2(<i>n</i> -6)/18:1(<i>n</i> -9)	$[M + 55\text{-FA}_{18:2}]^{+}$	$[M + 55\text{-FA}_{18:1}]^{+}$	0.2±0.0
TG 18:1(<i>n</i> -9)/18:1(<i>n</i> -9)/18:2(<i>n</i> -6)			0.4±0.0

^a The values have been averaged from five measurements (2-min records)

was modified with $\text{C}_3\text{H}_5\text{N}^{+}$. Therefore, only the two saturated acyls were cleaved off as neutral fatty acids (or ketenes as minor peaks). In the case of the regioisomer with both saturated chains in the outer positions (AOP), the intensity of $[M + 55\text{-FA}_{20:0}]^{+}$ and $[M + 55\text{-FA}_{16:0}]^{+}$ was roughly the same (Fig. 7a), whereas the isomer with arachidyl in the middle (PAO) eliminated arachidic acid less efficiently (Fig. 7b). In the full-scan APCI spectra of these regioisomers, the fragment intensities reflected the acyl positions as expected; the fragments corresponding to the acyl in the *sn*-2 position provided the peaks of the lowest intensities (Fig. 7c, d). Interestingly, the peak intensity ratio $[M + 55\text{-FA}_{20:0}]^{+}/[M + 55\text{-FA}_{16:0}]^{+}$ (Table 1) was exactly the same as the $[M + \text{H-FA}_{20:0}]^{+}/[M + \text{H-FA}_{16:0}]^{+}$ ratio calculated from the full-scan APCI spectrum

(the intensity ratio $[M + \text{H-FA}_{20:0}]^{+}/[M + \text{H-FA}_{16:0}]^{+}$ was 0.8 for AOP and 0.3 for PAO). In a regioisomeric pair 1,3-diolein-2-palmitin (TG 18:1(*n*-9)/16:0/18:1(*n*-9); OPO) and 1,2-diolein-3-palmitin (TG 18:1(*n*-9)/18:1(*n*-9)/16:0; OOP), Spectra S17 and S18, one of two oleyls was modified with $\text{C}_3\text{H}_5\text{N}^{+}$, likely with similar probability. Again, the neutral loss from the *sn*-2 position was less efficient as the ratio $[M + 55\text{-FA}_{18:1}]^{+}/[M + 55\text{-FA}_{16:0}]^{+}$ was significantly higher for OPO with both oleyls in the outer positions on glycerol (Table 1). Not surprisingly, the corresponding fragment intensity ratio was also significantly higher for OPO in the full-scan APCI spectra (the intensity ratio $[M + \text{H-FA}_{18:1}]^{+}/[M + \text{H-FA}_{16:0}]^{+}$ was 7.7 for OPO and 1.7 for OOP). The position of acyls on the glycerol backbone was also possible to follow in

Fig. 7 The zoomed regions of the APCI CID MS² spectra of the $[M + 55]^{+}$ adduct of 1-arachidin-2-olein-3-palmitin (TG 20:0/18:1(*n*-9)/16:0) (a) and 1-palmitin-2-arachidin-3-olein (TG 16:0/20:0/18:1(*n*-9)) (b). The zoomed regions of the APCI full-scan spectra of 1-arachidin-2-olein-3-palmitin (TG 20:0/18:1(*n*-9)/16:0) (c) and 1-palmitin-2-arachidin-3-olein (TG 16:0/20:0/18:1(*n*-9)) (d). The standard solution (20 μg/mL in chloroform) delivered by a syringe pump (20 μL/min) was mixed in a T-piece with acetonitrile (0.5 mL/min) and infused into the ion source (the spectrum averaged from a 2-min record)



the CID spectra of polyunsaturated TGs like in 1,2-olein-3-linolein (TG 18:1(*n*-9)/18:1(*n*-9)/18:2(*n*-6); OOL) and 1,3-olein-2-linolein (TG 18:1(*n*-9)/18:2(*n*-6)/18:1(*n*-9); OLO) (Spectra S42 and S43). However, as the probability of the C₃H₅N⁺⁺ adduct formation might be different for individual double bonds in various (poly)unsaturated chains, the fragment-ion ratios should be interpreted with caution. In this particular example, the neutral loss of linoleic acid was more efficient in the case of OOL (Table 1), which is again in agreement with the less efficient neutral loss from the *sn*-2 position.

Applications

The applicability of HPLC/APCI-MS² with [M + 55]⁺⁺ fragmentation in the ion trap for the comprehensive structural characterization of TGs in mixtures was assessed using olive oil and unsaturated TGs isolated from vernix caseosa. The TG molecular species were resolved using a proven method based on Nova-Pak C18 columns and an acetonitrile/propan-2-ol gradient [47, 19, 53]. There was no need to modify the separation conditions as acetonitrile in the mobile phase afforded the formation of the [M + 55]⁺⁺ adducts. The full-scan spectra provided molecular adducts and fragments useful for deducing the total number of carbons and double bonds in TG acyls [54]. The same information was possible to extract also from

the CID spectra of [M + 55]⁺⁺. The masses of the precursors determined the total number of carbons and double bonds. The fatty-acid neutral loss ions ([M + 55-FA]⁺⁺) were used for the determination of the number of carbon atoms and double bonds in acyls and the relative proportions of these ions reflected the positions of acyl on the glycerol backbone, like in case of [M + H-FA]⁺ in the full-scan spectra. Moreover, the CID MS/MS spectra provided information on the double-bond positions.

Table 2 shows the results on the olive oil sample obtained by the interpretation of the CID spectra of [M + 55]⁺⁺ only; the full-scan data were not used. For comparison purposes, the data were also interpreted in a classical way using the full-scan APCI spectra; the results summarized in the ESM (Table S1; Fig. S1) were in excellent agreement with a previously published report [47]. The interpretation of the CID spectra of [M + 55]⁺⁺ allowed us to gain information on double-bond positions in 20 TGs. Those were the most abundant TGs in the sample (93 % of the sample based on the peak areas); the spectra were interpretable even for TGs with the relative peak areas as low as 0.1 % in some cases. In the interpretation procedure, we focused on α ions labeled relative to the precursor ([M + 55]⁺⁺) mass. The α ions thus appeared at -29 Da, -43 Da, -57 Da, -71 Da, -85 Da, -99 Da, -113 Da etc., and indicated double bonds in the positions

Table 2 The unsaturated TGs identified in olive oil using CID of [M + 55]⁺⁺

R _t [min]	[M + 55] ⁺⁺	Fatty acid (neutral loss)	Double-bond position	TG ^a	ECN
65.0	933.5	18:2	<i>n</i> -6, <i>n</i> -9	18:2(<i>n</i> -6,9)/18:2(<i>n</i> -6,9)/18:2(<i>n</i> -6,9) ^b	42
65.8	933.5		<i>n</i> -9, <i>n</i> -6, <i>n</i> -3	18:1(<i>n</i> -9)_18:3(<i>n</i> -3,6,9)_18:2(<i>n</i> -6,9) ^c	42
71.2	935.8	18:1, 18:2	<i>n</i> -9, <i>n</i> -6	18:1(<i>n</i> -9)_18:2(<i>n</i> -6,9)_18:2(<i>n</i> -6,9) ^b	44
71.7	909.8	16:1, 18:1, 18:2	<i>n</i> -9, <i>n</i> -7, <i>n</i> -6	16:1(<i>n</i> -9)_18:1(<i>n</i> -9)_18:2(<i>n</i> -6,9)	44
71.9	935.6	18:1, 18:3	<i>n</i> -9, <i>n</i> -3	18:1(<i>n</i> -9)_18:1(<i>n</i> -9)_18:3(<i>n</i> -3,6,9)	44
72.6	909.5	16:0, 18:2	<i>n</i> -9, <i>n</i> -6	16:0_18:2(<i>n</i> -6, 9)_18:2(<i>n</i> -6, 9) ^b	44
73.4	909.6	16:0, 18:1, 18:3	<i>n</i> -9, <i>n</i> -3	16:0_18:1(<i>n</i> -9)_18:3(<i>n</i> -3,6,9)	44
77.0	937.7	18:1, 18:2	<i>n</i> -9, <i>n</i> -6	18:1(<i>n</i> -9)_18:1(<i>n</i> -9)_18:2(<i>n</i> -6,9)	46
77.6	911.6	16:1, 18:1	<i>n</i> -9, <i>n</i> -7	16:1(<i>n</i> -7)_18:1(<i>n</i> -9)_18:1(<i>n</i> -9)	46
78.5	911.6	16:0, 18:1, 18:2	<i>n</i> -9, <i>n</i> -7	16:0_18:1(<i>n</i> -9)_18:2(<i>n</i> -6, 9)	46
80.3	925.8	17:1, 18:1	<i>n</i> -9, <i>n</i> -8	17:1(<i>n</i> -8)_18:1(<i>n</i> -9)_18:1(<i>n</i> -9)	47
81.8	899.9	17:1	<i>n</i> -9, <i>n</i> -8	16:0_17:1(<i>n</i> -8)_18:1(<i>n</i> -9)	47
82.7	939.6	18:1	<i>n</i> -9	18:1(<i>n</i> -9)/18:1(<i>n</i> -9)/18:1(<i>n</i> -9) ^b	48
83.9	939.9		<i>n</i> -9, <i>n</i> -6	18:0_18:1(<i>n</i> -9)_18:2(<i>n</i> -6, 9) ^c	48
84.3	913.5	16:0, 18:1	<i>n</i> -9	16:0_18:1(<i>n</i> -9)_18:1(<i>n</i> -9) ^b	48
87.9	967.7	18:1, 20:1	<i>n</i> -9	18:1(<i>n</i> -9)_18:1(<i>n</i> -9)_20:1(<i>n</i> -9) ^b	50
89.1	967.7	18:1, 20:0	<i>n</i> -9	18:1(<i>n</i> -9)_18:2(<i>n</i> -6,9)_20:0	50
89.7	941.7		<i>n</i> -9	18:0_18:1(<i>n</i> -9)_18:1(<i>n</i> -9) ^c	50
94.6	969.7	18:1, 20:0	<i>n</i> -9	18:1(<i>n</i> -9)_18:1(<i>n</i> -9)_20:0 ^b	52

^a The most likely structures of TGs identified from the spectra

^b Unambiguously identified

^c The missing information on acyl composition has been taken from the full-scan spectrum

$n-3$, $n-4$, $n-5$, $n-6$, $n-7$, $n-8$, $n-9$, respectively. When the neutral radical already carried one double bond (i.e., another double bond existed closer to the chain terminus), the values were 2 mass units shifted. In the case of methylene-interrupted double bonds, the distances between α ions in the spectra were 40 Da. We clearly detected α ions corresponding to double bonds in monounsaturated acyls. In the case of polyunsaturated chains, we frequently observed only α ions indicating the outermost double bonds. If methylene-interrupted acyls were expected, this information was sufficient. However, an unequivocal interpretation of the spectra was not always possible even for a complete set of α ions. It is important to realize that the MS² spectra afforded cumulative information on double bonds in all three chains, without direct information on which chain the double bond existed. The double-bond assignment to a particular chain would be possible using MS³ performed with α ions or $[M + 55\text{-FA}]^{++}$ ions. Unfortunately, the MS³-spectra intensities were low, which makes their practical use hard to imagine. Nevertheless, the MS² alone might be sufficient for unambiguous double-bond localization in some cases. For instance, the peak in 71.2 min represented TG with one 18:1 and two 18:2 acyls (based on the $[M + 55]^{++}$ and $[M + 55\text{-FA}]^{++}$ masses) with the 18:2 chain in the *sn*-2 position (based on the $[M + 55\text{-FA}]^{++}$ fragment intensity ratio), see Fig. 8a. The α ions appeared at m/z

864.7 (-71 Da, $n-6$), m/z 822.6 (-113 Da, $n-9$), and m/z 824.6 (-111 Da, $n-9$ in an acyl with one additional double bond closer to the chain terminus). In this case, the interpretation was unequivocal: the double bonds $n-6$ and $n-9$ were in the doubly unsaturated acyls and $n-9$ is in the monounsaturated acyl. Therefore, the spectrum represented olein-dilinolein with linoleic acid in the *sn*-2 position (*cis* double bonds assumed). The spectral interpretation was also straightforward in the case of TGs with identical unsaturated acyls (e.g., the most abundant peak at the 82.2nd min with all double bonds in $n-9$, identified as triolein, or the peak at the 84.3rd min with one C16:0 and two $n-9$ C18:1 chains, interpreted as palmitin-diolein). In several minor TGs, we were not able to detect the $[M + 55\text{-FA}]^{++}$ fragments reliably, but we clearly saw α ions, enabling us to localize the positions of double bonds.

Vernix caseosa lipids are known as an extremely complex mixture of various lipids with branched and unsaturated chains [55]. TGs of vernix caseosa consist of an exceptionally large number of molecular species, which makes their analysis particularly challenging. A comprehensive analysis of all TGs in vernix caseosa was not attempted in this work and the data were interpreted only partially. The α fragments mostly showed a double bond up to $n-12$, but small peaks in some spectra also indicated double bonds at more distant positions from the chain termini. Figure 8b shows a spectrum for a peak at the 70.0th min (see the basepeak chromatogram in ESM Fig. S2). The spectrum represents a mixture of TGs with two saturated fatty acyls (14:0, 15:0, or 16:0) and one monounsaturated acyl (14:1, 15:1, 16:1, or 17:1) with double bonds mainly in $n-10$ and $n-8$. The results indicated the feasibility of the localization of double bonds in the TGs of vernix caseosa; however, a reliable and comprehensive analysis cannot be achieved without substantial improvement of the separation method. As the concentration of acetonitrile in the mobile phase gradually decreased in the course of the analysis, TGs with high ECN values were ionized at low concentrations of acetonitrile. Consequently, the efficiency of the $[M + 55]^{++}$ formation was reduced and the MS² spectra were of rather poor quality at higher retention times. The concentration of acetonitrile during ionization might be increased by a post-column addition of acetonitrile, but this approach was not tested in this work.

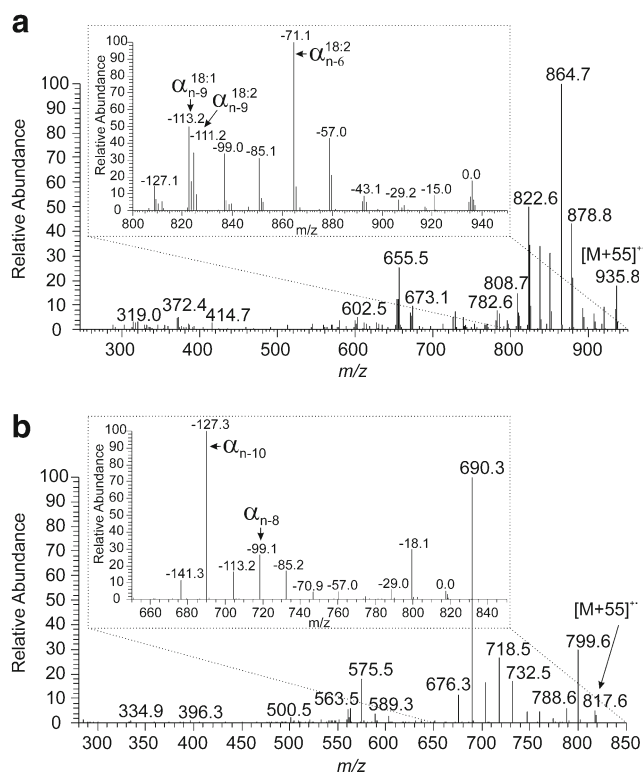


Fig. 8 The APCI CID MS² spectra of the TG $[M + 55]^{++}$ adduct taken across the chromatographic peak ($t_R=71.2$ min) in the olive oil sample and interpreted as 18:1($n-9$), 18:2($n-6,9$), 18:2($n-6,9$) (a) and the chromatographic peak ($t_R=70.0$ min) in the vernix caseosa sample (b). For experimental conditions, see the “Material and methods” section

Conclusions

The results in this work have proven that acetonitrile-related $[M + 55]^{++}$ ions formed in APCI source are useful for the structure elucidation of TGs. The fragmentation spectra of these ions provided information on (i) the total number of carbons and double bonds in the whole molecule (the mass of the $[M + 55]^{++}$ precursor), (ii) the number of carbons and

double bonds in acyls (masses of the $[M + 55\text{-FA}]^{+}$ fragments), (iii) the acyl in the *sn*-2 position on the glycerol backbone (the intensity ratios of the $[M + 55\text{-FA}]^{+}$ fragments), and (iv) the double-bond positions in acyls (the masses of the α and ω ions). The $[M + 55]^{+}$ ions were generated under the common conditions used for the separation of TGs on classical HPLC columns, i.e., in the mobile phases containing acetonitrile and submilliliter per minute flow rates. Therefore, it is not difficult to adapt the existing HPLC/APCI-MS methods for the localization of double bonds. The fragmentation of $[M + 55]^{+}$ was achieved in the ion trap using either CID or PQD. Although PQD afforded for each double bond two diagnostic ions and CID only one, the CID was preferred because of its higher sensitivity. Although the fragmentation spectra of $[M + 55]^{+}$ usually provide all information for characterizing TG structures, such spectra are better to be used for double-bond localization only; all the other information is more easily accessible from the full-scan spectra. The MS² spectra of $[M + 55]^{+}$ generally contained diagnostic peaks for all (or most) of the double bonds in the molecule. Yet in the case of unknowns, the interpretation was not always straightforward. The MS² spectra contained cumulative information on all double bonds in all three acyls, which complicated or even hindered a correct assignment of particular signals. This limitation would likely have been solved by the use of MS³, but the sensitivity was an issue. Despite the limitations discussed above, the method is an easy way of determining double bonds in TGs, which has been demonstrated with a large set of standards and also for natural samples.

Acknowledgments This work was financially supported by the Czech Science Foundation (Project No. P206/12/0750), the Academy of Sciences of the Czech Republic (RVO 61388963) and Charles University in Prague (Project SVV). The authors thank Dr. Miroslav Lísa for advices with the randomization synthesis.

References

- Gunstone FD, Harwood JL, Dijkstra AJ (2007) The lipid handbook 3 edn. CRC, Boca Raton
- Holčapek M, Jandera P, Fischer J, Prokeš B (1999) Analytical monitoring of the production of biodiesel by high-performance liquid chromatography with various detection methods. *J Chromatogr A* 858(1):13–31
- Fauconnot L, Hau J, Aeschlimann JM, Fay LB, Dionisi F (2004) Quantitative analysis of triacylglycerol regioisomers in fats and oils using reversed-phase high-performance liquid chromatography and atmospheric pressure chemical ionization mass spectrometry. *Rapid Commun Mass Spectrom* 18(2):218–224. doi:10.1002/rcm.1317
- Cvačka J, Hovorka O, Jiroš P, Kindl J, Stránský K, Valterová I (2006) Analysis of triacylglycerols in fat body of bumblebees by chromatographic methods. *J Chromatogr A* 1101(1–2):226–237. doi:10.1016/j.chroma.2005.10.001
- Sandra K, Pereira AD, Vanhoenacker G, David F, Sandra P (2010) Comprehensive blood plasma lipidomics by liquid chromatography/quadrupole time-of-flight mass spectrometry. *J Chromatogr A* 1217(25):4087–4099. doi:10.1016/j.chroma.2010.02.039
- Laakso P, Voutilainen P (1996) Analysis of triacylglycerols by silver-ion high-performance liquid chromatography—atmospheric pressure chemical ionization mass spectrometry. *Lipids* 31(12):1311–1322. doi:10.1007/bf02587918
- Lísa M, Velínská H, Holčapek M (2009) Regioisomeric characterization of triacylglycerols using silver-ion HPLC/MS and randomization synthesis of standards. *Anal Chem* 81(10):3903–3910. doi:10.1021/ac900150j
- Lísa M, Holčapek M (2013) Characterization of triacylglycerol enantiomers using chiral HPLC/APCI-MS and synthesis of enantiomeric triacylglycerols. *Anal Chem* 85(3):1852–1859. doi:10.1021/ac303237a
- Dugo P, Kumm T, Crupi ML, Cotroneo A, Mondello L (2006) Comprehensive two-dimensional liquid chromatography combined with mass spectrometric detection in the analyses of triacylglycerols in natural lipidic matrixes. *J Chromatogr A* 1112(1–2):269–275. doi:10.1016/j.chroma.2005.10.070
- van der Klift EJC, Vivo-Truyols G, Claassen FW, van Holthoorn FL, van Beek TA (2008) Comprehensive two-dimensional liquid chromatography with ultraviolet, evaporative light scattering and mass spectrometric detection of triacylglycerols in corn oil. *J Chromatogr A* 1178(1–2):43–55. doi:10.1016/j.chroma.2007.11.039
- Perrin JL, Naudet M (1983) Identification and determination of triglycerides in natural fats by high-performance liquid-chromatography. *Revue Francaise Des Corps Gras* 30(7–8):279–285
- Hsu FF, Turk J (1999) Structural characterization of triacylglycerols as lithiated adducts by electrospray ionization mass spectrometry using low-energy collisionally activated dissociation on a triple stage quadrupole instrument. *J Am Soc Mass Spectrom* 10(7):587–599. doi:10.1016/s1044-0305(99)00035-5
- Holčapek M, Jandera P, Zderadička P, Hrubá L (2003) Characterization of triacylglycerol and diacylglycerol composition of plant oils using high-performance liquid chromatography-atmospheric pressure chemical ionization mass spectrometry. *J Chromatogr A* 1010(2):195–215. doi:10.1016/s0021-9673(03)01030-6
- Han XL, Gross RW (2003) Global analyses of cellular lipidomes directly from crude extracts of biological samples by ESI mass spectrometry: a bridge to lipidomics. *J Lipid Res* 44(6):1071–1079. doi:10.1194/jlr.R300004-JLR200
- Byrdwell WC (2001) Atmospheric pressure chemical ionization mass spectrometry for analysis of lipids. *Lipids* 36(4):327–346. doi:10.1007/s11745-001-0725-5
- Cai SS, Syage JA (2006) Comparison of atmospheric pressure photoionization, atmospheric pressure chemical ionization, and electrospray ionization mass spectrometry for analysis of lipids. *Anal Chem* 78(4):1191–1199. doi:10.1021/ac0515834
- Asbury GR, Al-Saad K, Siems WF, Hannan RM, Hill HH (1999) Analysis of triacylglycerols and whole oils by matrix-assisted laser desorption/ionization time of flight mass spectrometry. *J Am Soc Mass Spectrom* 10(10):983–991. doi:10.1016/s1044-0305(99)00063-x
- Pittenauer E, Allmaier G (2009) The renaissance of high-energy CID for structural elucidation of complex lipids: MALDI-TOF/RTOF-MS of alkali cationized triacylglycerols. *J Am Soc Mass Spectrom* 20(6):1037–1047. doi:10.1016/j.jasms.2009.01.009
- Kofronová E, Cvačka J, Vrkoslav V, Hanus R, Jiroš P, Kindl J, Hovorka O, Valterová I (2009) A comparison of HPLC/APCI-MS and MALDI-MS for characterising triacylglycerols in insects: species-specific composition of lipids in the fat bodies of bumblebee males. *J Chromatogr B-Anal Technol Biomed Life Sci* 877(30):3878–3884. doi:10.1016/j.jchromb.2009.09.040
- Suni NM, Aalto H, Kauppila TJ, Kotiaho T, Kostianen R (2012) Analysis of lipids with desorption atmospheric pressure

- photoionization-mass spectrometry (DAPPI-MS) and desorption electrospray ionization-mass spectrometry (DESI-MS). *J Mass Spectrom* 47(5):611–619. doi:10.1002/jms.2992
21. Cheng CF, Gross ML (1998) Complete structural elucidation of triacylglycerols by tandem sector mass spectrometry. *Anal Chem* 70(20):4417–4426. doi:10.1021/ac9805192
 22. Lauer WM, Aasen AJ, Graff G, Holman RT (1970) Mass spectrometry of lipids. 5. Mass spectrometry of triglycerides. 1. Structural effects. *Lipids* 5(11):861–868. doi:10.1007/bf02531117
 23. Games DE (1978) Soft ionization mass-spectral methods for lipid analysis. *Chem Phys Lipids* 21(4):389–402. doi:10.1016/0009-3084(78)90048-8
 24. Thomas MC, Mitchell TW, Harman DG, Deeley JM, Murphy RC, Blanksby SJ (2007) Elucidation of double bond position in unsaturated lipids by ozone electrospray ionization mass spectrometry. *Anal Chem* 79(13):5013–5022. doi:10.1021/ac0702185
 25. Xu Y, Brenna JT (2007) Atmospheric pressure covalent adduct chemical ionization tandem mass spectrometry for double bond localization in monoene- and diene-containing triacylglycerols. *Anal Chem* 79(6):2525–2536. doi:10.1021/ac062055a
 26. Thomas MC, Mitchell TW, Harman DG, Deeley JM, Nealon JR, Blanksby SJ (2008) Ozone-induced dissociation: elucidation of double bond position within mass-selected lipid ions. *Anal Chem* 80(1):303–311. doi:10.1021/ac7017684
 27. Hsu F-F, Turk J (2010) Electrospray ionization multiple-stage linear ion-trap mass spectrometry for structural elucidation of triacylglycerols: assignment of fatty acyl groups on the glycerol backbone and location of double bonds. *J Am Soc Mass Spectrom* 21(4):657–669. doi:10.1016/j.jasms.2010.01.007
 28. Brown SHJ, Mitchell TW, Blanksby SJ (2011) Analysis of unsaturated lipids by ozone-induced dissociation. *Biochim Biophys Acta-Mol Cell Biol Lipids* 1811(11):807–817. doi:10.1016/j.bbalip.2011.04.015
 29. Vrkoslav V, Háková M, Pecková K, Urbanová K, Cvačka J (2011) Localization of double bonds in wax esters by high-performance liquid chromatography/atmospheric pressure chemical ionization mass spectrometry utilizing the fragmentation of acetonitrile-related adducts. *Anal Chem* 83(8):2978–2986. doi:10.1021/ac1030682
 30. Pham HT, Ly T, Trevitt AJ, Mitchell TW, Blanksby SJ (2012) Differentiation of complex lipid isomers by radical-directed dissociation mass spectrometry. *Anal Chem* 84(17):7525–7532. doi:10.1021/ac301652a
 31. Moneti G, Pieraccini G, Dani F, Turillazzi S, Favretto D, Traldi P (1997) Ion-molecule reactions of ionic species from acetonitrile with unsaturated hydrocarbons for the identification of the double-bond position using an ion trap. *J Mass Spectrom* 32(12):1371–1373. doi:10.1002/(sici)1096-9888(199712)32:12<1371::aid-jms588>3.0.co;2-e
 32. Moneti G, Pieraccini G, Favretto D, Traldi P (1998) Acetonitrile in chemical ionization of monounsaturated hydrocarbons: a C-13 and H-2 labeling study. *J Mass Spectrom* 33(11):1148–1149. doi:10.1002/(sici)1096-9888(199811)33:11<1148::aid-jms707>3.0.co;2-y
 33. Moneti G, Pieraccini G, Favretto D, Traldi P (1999) Reactions of ionic species from acetonitrile with long-chain saturated and unsaturated alcohols. *J Mass Spectrom* 34(12):1354–1360. doi:10.1002/(sici)1096-9888(199912)34:12<1354::aid-jms894>3.0.co;2-1
 34. Oldham NJ, Svatoš A (1999) Determination of the double bond position in functionalized monoenes by chemical ionization ion-trap mass spectrometry using acetonitrile as a reagent gas. *Rapid Commun Mass Spectrom* 13(5):331–336. doi:10.1002/(sici)1097-0231(19990315)13:5<331::aid-rcm487>3.3.co;2-1
 35. Van Pelt CK, Carpenter BK, Brenna JT (1999) Studies of structure and mechanism in acetonitrile chemical ionization tandem mass spectrometry of polyunsaturated fatty acid methyl esters. *J Am Soc Mass Spectrom* 10(12):1253–1262
 36. Van Pelt CK, Brenna JT (1999) Acetonitrile chemical ionization tandem mass spectrometry to locate double bonds in polyunsaturated fatty acid methyl esters. *Anal Chem* 71(10):1981–1989. doi:10.1021/ac981387f
 37. Van Pelt CK, Huang MC, Tschanz CL, Brenna JT (1999) An octaene fatty acid, 4,7,10,13,16,19,22,25-octacosaoctanoic acid (28: 8*n*-3), found in marine oils. *J Lipid Res* 40(8):1501–1505
 38. Michaud AL, Diau GY, Abril R, Brenna JT (2002) Double bond localization in minor homoallylic fatty acid methyl esters using acetonitrile chemical ionization tandem mass spectrometry. *Anal Biochem* 307(2):348–360. doi:10.1016/s0003-2697(02)00037-4
 39. Michaud AL, Yurawecz MP, Delmonte P, Corl BA, Bauman DE, Brenna JT (2003) Identification and characterization of conjugated fatty acid methyl esters of mixed double bond geometry by acetonitrile chemical ionization tandem mass spectrometry. *Anal Chem* 75(18):4925–4930. doi:10.1021/ac034221+
 40. Michaud AL, Lawrence P, Adlof R, Brenna JT (2005) On the formation of conjugated linoleic acid diagnostic ions with acetonitrile chemical ionization tandem mass spectrometry. *Rapid Commun Mass Spectrom* 19(3):363–368. doi:10.1002/rcm.1797
 41. Lawrence P, Brenna JT (2006) Acetonitrile covalent adduct chemical ionization mass spectrometry for double bond localization in non-methylene-interrupted polyene fatty acid methyl esters. *Anal Chem* 78(4):1312–1317. doi:10.1021/ac0516584
 42. Gomez-Cortes P, Tyburczy C, Brenna JT, Juarez M, Angel de la Fuente M (2009) Characterization of *cis*-9 *trans*-11 *trans*-15 C18:3 in milk fat by GC and covalent adduct chemical ionization tandem MS. *J Lipid Res* 50(12):2412–2420. doi:10.1194/jlr.M800662-JLR200
 43. Alves SP, Tyburczy C, Lawrence P, Bessa RJB, Brenna JT (2011) Acetonitrile covalent adduct chemical ionization tandem mass spectrometry of non-methylene-interrupted pentaene fatty acid methyl esters. *Rapid Commun Mass Spectrom* 25(14):1933–1941. doi:10.1002/rcm.5065
 44. Oldham NJ (1999) Ion/molecule reactions provide new evidence for the structure and origin of C₃H₄N⁺ from acetonitrile chemical ionization plasma. *Rapid Commun Mass Spectrom* 13(16):1694–1698. doi:10.1002/(sici)1097-0231(19990830)13:16<1694::aid-rcm702>3.0.co;2-1
 45. Vrkoslav V, Cvačka J (2012) Identification of the double-bond position in fatty acid methyl esters by liquid chromatography/atmospheric pressure chemical ionisation mass spectrometry. *J Chromatogr A* 1259:244–250. doi:10.1016/j.chroma.2012.04.055
 46. Šubčíková L, Hoskovec M, Vrkoslav V, Čmelíková T, Háková E, Míková R, Coufal P, Doležal A, Plavka R, Cvačka J (2015) Analysis of 1,2-diol diesters in vermic caseosa by high-performance liquid chromatography—atmospheric pressure chemical ionization mass spectrometry. *J Chromatogr A* 1378:8–18. doi:10.1016/j.chroma.2014.11.075
 47. Lisa M, Holčápek M, Boháč M (2009) Statistical evaluation of triacylglycerol composition in plant oils based on high-performance liquid chromatography-atmospheric pressure chemical ionization mass spectrometry data. *J Agric Food Chem* 57(15):6888–6898. doi:10.1021/jf901189u
 48. Liebisch G, Vizcaino JA, Koefeler H, Troetzmueller M, Griffiths WJ, Schmitz G, Spener F, Wakelam MJO (2013) Shorthand notation for lipid structures derived from mass spectrometry. *J Lipid Res* 54(6):1523–1530. doi:10.1194/jlr.M033506
 49. Rousseau D, Marangoni AG (2002) In: Akoh CC, Min DB (eds) *Food lipids: chemistry, nutrition, and biotechnology*, 2nd edn. CRC, New York

50. Mottram HR, Evershed RP (1996) Structure analysis of triacylglycerol positional isomers using atmospheric pressure chemical ionisation mass spectrometry. *Tetrahedron Lett* 37(47):8593–8596. doi:[10.1016/0040-4039\(96\)01964-8](https://doi.org/10.1016/0040-4039(96)01964-8)
51. Laakso P (2002) Mass spectrometry of triacylglycerols. *Eur J Lipid Sci Technol* 104(1):43–49. doi:[10.1002/1438-9312\(200201\)104:1<43::AID-EJLT43>3.0.CO;2-J](https://doi.org/10.1002/1438-9312(200201)104:1<43::AID-EJLT43>3.0.CO;2-J)
52. Baiocchi C, Medana C, Dal Bello F, Giancotti V, Aigotti R, Gastaldi D (2015) Analysis of regioisomers of polyunsaturated triacylglycerols in marine matrices by HPLC/HRMS. *Food Chem* 166:551–560. doi:[10.1016/j.foodchem.2014.06.067](https://doi.org/10.1016/j.foodchem.2014.06.067)
53. Kofroňová E, Cvačka J, Jiroš P, Sýkora D, Valterová I (2009) Analysis of insect triacylglycerols using liquid chromatography-atmospheric pressure chemical ionization-mass spectrometry. *Eur J Lipid Sci Technol* 111:519–525. doi:[10.1002/ejlt.200800228](https://doi.org/10.1002/ejlt.200800228)
54. Cvačka J, Krafková E, Jiroš P, Valterová I (2006) Computer-assisted interpretation of atmospheric pressure chemical ionization mass spectra of triacylglycerols. *Rapid Commun Mass Spectrom* 20(23):3586–3594. doi:[10.1002/rcm.2770](https://doi.org/10.1002/rcm.2770)
55. Rissmann R, Groenink HWW, Weerheim AM, Hoath SB, Ponc M, Bouwstra JA (2006) New insights into ultrastructure, lipid composition and organization of vernix caseosa. *J Invest Dermatol* 126(8):1823–1833. doi:[10.1038/sj.jid.5700305](https://doi.org/10.1038/sj.jid.5700305)